Romanian Reports in Physics **78**, 103 (2026)

A SPECTRAL APPROACH FOR MULTI-DIMENSIONAL NON-LINEAR DISTRIBUTED CONVECTION-DIFFUSION EQUATIONS

A. EMIN[1,a], M.A. ABDELKAWY[2,b], D. BALEANU[3,4,c]

[1]Department of Software Engineering, Istanbul Gelisim University, 34310, Istanbul, Turkey
[a]Email: *azm.amin@yahoo.com*
[2]Department of Mathematics and Statistics, College of Science, Imam Mohammad Ibn Saud Islamic University (IMSIU), Riyadh, Saudi Arabia
[b]Email: *maohamed@imamu.edu.sa*
[3]Department of Computer Science and Mathematics, Lebanese American University, Beirut, Lebanon
[4]Institute of Space Sciences-subsidiary of INFLPR, Magurele-Bucharest, Romania
[c]Corresponding author, Email: *dumitru.baleanu@lau.edu.lb*

Received July 20, 2025

Abstract. This study presents a Romanovski–Jacobi (R-J) spectral collocation method for the numerical approximation of solutions to multi-dimensional non-linear distributed-order fractional convection-diffusion equations (DOFCDEs). Due to the inherent analytical intractability of such equations, the necessity for robust numerical approaches is underscored. The proposed method leverages the spectral efficiency of R-J polynomials to construct an accurate collocation scheme tailored for non-linear DOFCDEs. Emphasis is placed on the crucial role of advanced numerical computation in addressing complex phenomena governed by distributed-order fractional dynamics. The efficacy and accuracy of the proposed technique are validated through the successful resolution of four representative test problems, demonstrating its potential for reliable simulation and analysis of fractional systems.

Key words: Caputo fractional derivative; Romanovski–Jacobi polynomials; Collocation method; Distributed fractional convection-diffusion equations.

DOI: https://doi.org/10.59277/RomRepPhys.2026.78.103

1. INTRODUCTION

Differential equations serve as a foundational tool in mathematical modeling across various disciplines, including physics [1], engineering [2], biology [3], and finance [4]. Traditionally, these models are formulated using integer-order derivatives, which represent the number of successive differentiations of a function. However, numerous real-world phenomena exhibit complex behaviors such as anomalous diffusion, memory effects, and spatial non-locality – that are inadequately captured by classical integer-order models. To address these limitations, there has been a growing interest in fractional calculus, which generalizes the concept of differentiation and integration to non-integer (fractional) orders. This extension has proven particularly

effective for capturing the dynamics of systems governed by non-local and history-dependent processes [5, 6]. Within this context, fractional differential equations have emerged as a powerful mathematical framework for modeling such intricate physical systems; see, for example, the recent works [7–11].

Fractional distributed-order differential equations represent a class of complex systems characterized by non-integer order derivatives and non-local interactions. Owing to their analytical intractability, various numerical techniques have been developed to approximate their solutions, including finite difference, finite element, meshless, and spectral methods.

Finite difference methods [12, 13] discretize the time and space domains to approximate the governing equations using difference quotients. Finite element approaches [14–16] decompose the computational domain into subregions and employ piecewise polynomial basis functions for spatial approximation. Spectral methods [17, 18], by contrast, utilize global orthogonal basis functions to achieve high-accuracy approximations and exponential convergence rates. Among these, orthogonal polynomial families such as Legendre and Jacobi polynomials are commonly employed. Meshless techniques [19, 20], including the method of fundamental solutions (MFS) and radial basis function (RBF) interpolation, are particularly effective in handling complex geometries and irregular boundary conditions without the need for mesh generation. Collectively, these computational methods play a crucial role in the numerical investigation of systems exhibiting memory effects, anomalous diffusion, and spatial heterogeneity.

Gao and Sun [21] introduced two discrete methods for solving distributed-order (D-O) fractional wave equations, while in [22], they developed two difference schemes for addressing D-O differential equations, applicable in both one- and two-dimensional domains. Chen [23] investigated the numerical approximation of the fractional reaction-diffusion equation of D-O time, employing finite difference methods and spectral approximation *via* Laguerre functions for spatial discretization. Heydari [24] presented a set of coupled Klein–Gordon–Schrödinger fractional D-O equations, incorporating a fractional D-O derivative formulated using Caputo fractional differentiation. Rahimkhani [25] applied Chelyshkov wavelets to solve D-O fractional differential equations. Additionally, Saifullah *et al.* [26] addressed the non-linear Klein–Gordon problem by employing a combination of the decomposition method.

Spectral methods, as discussed by [27, 28], have been widely employed across various disciplines for over four decades. Initially applied in simpler scenarios involving periodic boundary conditions and basic geometries, Fourier-based spectral techniques have experienced substantial theoretical developments, making them increasingly effective for solving complex problems. These methods are known for their superior accuracy and exponential convergence rates, outperforming other nu-

merical approaches. Several spectral techniques have been developed, including collocation [29], tau [30], Petrov–Galerkin [31], and Galerkin [32], with coefficients optimized to minimize absolute errors. In particular, spectral collocation methods offer highly accurate approximations of solutions to differential equations, with residuals approaching zero at selected points. This technique has demonstrated its utility in numerous scientific and engineering applications due to its notable advantages.

The primary objective of this article is to apply the Romanovski–Jacobi spectral collocation (RJSC) method for approximating distributed-order fractional differential equations (DOFDEs). To obtain a numerical solution, the residuals of the problem are computed through a finite expansion. By enforcing appropriate initial and boundary conditions, the method yields more accurate numerical results that are both reliable and consistent.

The structure of the paper is as follows. Section 2 introduces fundamental concepts and reviews key properties of R-J polynomials. Section 3 addresses the solution of one-dimensional (1D) non-linear DOFCDEs, while Sec. 4 solves 2D non-linear DOFCDEs. Section 5 presents numerical problems that demonstrate the effectiveness and accuracy of the proposed methods. Finally, Sec. 6 summarizes the conclusions drawn from the results and discusses the implications of the findings.

2. FUNDAMENTAL CONCEPTS

2.1. FRACTIONAL CALCULUS

This Section defines the fundamental terms and concepts that will be used throughout the subsequent Sections.

Definition 2.1 ([33]) The right and left Caputo fractional derivatives D^{α_1} of order α_1

$$D_{+}^{\alpha_1}\mathcal{Y}(\vartheta)=\frac{1}{\Gamma(\eta-\alpha_1)}\left(\int_0^{\vartheta}(\vartheta-\kappa)^{\eta-\alpha_1-1}\mathcal{Y}^{(\eta)}(\kappa)d\kappa\right),\quad \eta-1<\alpha_1\leq\eta,\ \vartheta>0. \tag{1}$$

$$D_{-}^{\alpha_1}\mathcal{Y}(\vartheta)=\frac{(-1)^{\eta}}{\Gamma(\eta-\alpha_1)}\left(\int_{\vartheta}^{L}(\kappa-\vartheta)^{\eta-\alpha_1-1}\mathcal{Y}^{(\eta)}(\kappa)d\kappa\right),\quad \eta-1<\alpha_1\leq\eta,\ \vartheta>0. \tag{2}$$

The operator $D_{\pm}^{\alpha_1}$ has the subsequent property:

$$D_{\pm}^{\alpha_1}I_{\pm}^{\alpha_1}\mathcal{Y}(\kappa)=\mathcal{Y}(\kappa)I_{\pm}^{\alpha_1}D_{\pm}^{\alpha_1}\mathcal{Y}(\kappa)=-\sum_{\omega_1=0}^{\lceil\alpha_1\rceil-1}\mathcal{Y}^{(\omega_1)}(0^{+})\frac{\kappa^{\omega_1}}{\omega_1!}+\mathcal{Y}(\kappa), \tag{3}$$

$D_{\pm}^{\alpha_1}$ and $I_{\pm}^{\alpha_1}$ are the operator values for both the left and right Caputo differentials

and the integrals, respectively.

Definition 2.2 ([33]) For the fractional integrals with order $\alpha_1 > 0$, the right- and left-sided formulations are:

$$I_{+}^{\alpha_1}\mathcal{Y}(\vartheta) = \frac{1}{\Gamma(\alpha_1)}\int_0^{\vartheta}(\vartheta-\kappa)^{\alpha_1-1}\mathcal{Y}(\kappa)d\kappa, \tag{4}$$

$$I_{-}^{\alpha_1}\mathcal{Y}(\vartheta) = \frac{1}{\Gamma(\alpha_1)}\int_{\vartheta}^{L}(m-\vartheta)^{\alpha_1-1}\mathcal{Y}(m)dm. \tag{5}$$

2.2. THE R-J POLYNOMIALS

The RJSC technique proves highly effective for solving distributed-order fractional convection-diffusion equations (DOFCDEs) due to its scalability and sensitivity to variable modifications, particularly when employing Jacobi polynomials. These methods efficiently handle problems of increasing size or complexity while maintaining high performance, as approximation accuracy improves with an increased number of collocation points. RJSC approaches enable analysis of nonlinear DOFCDEs across multiple scales from localized dynamics to large-scale systems while preserving computational efficiency.

The strength of these techniques lies in the flexibility and robustness of Jacobi polynomials, which accommodate parametric variations and adapt seamlessly to different forms of fractional differential equations with variable characteristics. By systematically adjusting the parameters of the Jacobi polynomials, researchers can enhance both the convergence rate and the accuracy of the numerical solutions, thereby significantly improving the overall effectiveness of the method.

Definition 2.3 ([34]) The Romanovski polynomials (RPs) with degree i and of form (ρ_1, σ_1) indicate with $\hat{\mathcal{R}}_{\ell}^{(\rho_1,\sigma_1)}$ and are defined

$$\hat{\mathcal{R}}_{\ell}^{(\rho_1,\sigma_1)} := \frac{(\rho_1+1)_{\ell}}{\ell!}{}_2F_1(-\ell, \ell+\rho_1+\sigma_1+1; \rho_1+1, \varrho). \tag{6}$$

Using the provided values $\rho_1 > -1$ and $\sigma_1 < -2\mathcal{M} - \rho_1 - 1$, the explicit equation following may be utilized for generating the collocation comprising $(\mathcal{M}+1)$ amount of the one-dimensional RJPs on $[0, \infty)$:

$$\hat{\mathcal{R}}_{\ell}^{(\rho_1,\sigma_1)}(\varrho) = \sum_{k=0}^{\ell}\frac{(-1)^k\left(\Gamma(\ell+\rho_1+1)\Gamma(-\ell-\rho_1-\sigma_1)\right)}{k!\Gamma(\ell-k+1)\Gamma(k+\rho_1+1)\Gamma(-\ell-k-\rho_1-\sigma_1)}\varrho^k, \ell = 0, ..., \mathcal{M}. \tag{7}$$

On the range $[0, \infty]$, the Romanovski–Jacobi polynomials (R-JPs), given as $\hat{\mathcal{R}}_{\ell}^{(\rho_1,\sigma_1)}(\varrho)$, are orthogonal with regard to the weight function $\mathrm{W}(\varrho) = \varrho^{\rho_1}(1+\chi)^{\sigma_1}$.

Their criteria for orthogonality is as follows:

$$\int_0^\infty \hat{\mathcal{R}}_n^{(\rho_1,\sigma_1)}(\chi)\hat{\mathcal{R}}_m^{(\rho_1,\sigma_1)}(\chi)w(\chi)\,d\chi = h_n\delta_{nm},$$

where $h_\ell = \frac{\Gamma(\ell+\rho_1+1)\Gamma(-\ell-\rho_1-\sigma_1)}{\Gamma(2\ell+\rho_1+\sigma_1+1)\ell!\Gamma(-\ell-\sigma_1)}$ is a normalization constant.

Theorem 2.1 Consider $\rho_1 > -1$ and $\rho_1+\sigma_1+N+1<0$. For $0\le \ell, m \le \frac{N}{2}$, the RPs [34]

$$\int_0^\infty \hat{\mathcal{R}}_\ell^{(\rho_1,\sigma_1)}(\varrho)\hat{\mathcal{R}}_m^{(\rho_1,\sigma_1)}(\varrho)w_{\rho_1,\sigma_1}(\varrho)\,dt = (-1)^{\ell+1}\frac{\Gamma(-\ell-\rho_1-\sigma_1)\Gamma(\ell+\rho_1+1)(\sigma_1+1)_\ell}{\ell!(2\ell+\rho_1+\sigma_1+1)\Gamma(-\sigma_1)}\delta_{\ell m}, \tag{8}$$

where the weight function is $w_{\rho_1,\sigma_1}(\varrho) = \varrho^{\rho_1}(1+\varrho)^{\sigma_1}$.

The relation between the Jacobi $\hat{\mathcal{J}}_\ell^{(\rho_1,\sigma_1)}(\varrho)$ and the RPs $\hat{\mathcal{R}}_\ell^{(\rho_1,\sigma_1)}(\varrho)$ is given by

$$\hat{\mathcal{R}}_\ell^{(\rho_1,\sigma_1)}(\varrho) = \hat{\mathcal{J}}_\ell^{(\rho_1,\sigma_1)}(1+2\varrho), \tag{9}$$

the explicit description of RPs is expressed *via*

$$\hat{\mathcal{R}}_\ell^{(\rho_1,\sigma_1)}(\varrho) := \sum_{m=0}^{\ell} a_{\ell,m}^{(\rho_1,\sigma_1)}\varrho^m, \quad a_{\ell,m}^{(\rho_1,\sigma_1)} = \binom{\ell+\rho_1+\sigma_1+m}{m}\binom{\ell+\rho_1}{\ell-m}. \tag{10}$$

R-JPs are eigenfunctions of the Sturm–Liouville operator $\mathcal{L}_{\rho_1,\sigma_1}$ is defined as:

$$\begin{aligned}\mathcal{L}_{\rho_1,\sigma_1}u :&= \varrho(1+\varrho)\partial_\varrho^2 u(\varrho) + ((2+\rho_1+\sigma_1)\varrho + (1+\rho_1))\partial_\varrho u(\varrho)\\ &= \varrho^{-\rho_1}(1+\varrho)^{-\sigma_1}\partial_\varrho(\varrho^{\rho_1+1}(1+\varrho)^{\rho_1+1}\partial_\varrho u(\varrho)).\end{aligned} \tag{11}$$

Lemma 2.2 The following recursive relationship applies to the one-dimensional R-JPs [35]

$$\begin{cases}\hat{\mathcal{R}}_{\ell+1}^{(\rho_1,\sigma_1)}(\varrho) = \big(A_\ell^{(\rho_1,\sigma_1)}(\varrho) - B_\ell^{(\rho_1,\sigma_1)}\big)\hat{\mathcal{R}}_\ell^{(\rho_1,\sigma_1)}(\varrho) - C_\ell^{(\rho_1,\sigma_1)}\hat{\mathcal{R}}_{\ell-1}^{(\rho_1,\sigma_1)}(\varrho), \quad \ell\le 1,\\ \hat{\mathcal{R}}_0^{(\rho_1,\sigma_1)}(\varrho) = 1,\\ \hat{\mathcal{R}}_1^{(\rho_1,\sigma_1)}(\varrho) = (\rho_1+\sigma_1+2)\varrho+\rho_1+1,\end{cases} \tag{12}$$

where

$$\begin{cases}A_\ell^{(\rho_1,\sigma_1)} = \frac{(2\ell+\rho_1+\sigma_1+1)(2\ell+\rho_1+\sigma_1+2)}{(\ell+1)(\ell+\rho_1+\sigma_1+1)},\\ B_\ell^{(\rho_1,\sigma_1)} = -\frac{(2\ell+\rho_1+\sigma_1+1)(2\ell(\ell+1)+(\rho_1+\sigma_1)(\rho_1+2\ell+1))}{(\ell+1)(\ell+\rho_1+\sigma_1+1)(2\ell+\rho_1+\sigma_1)},\\ C_\ell^{(\rho_1,\sigma_1)} = \frac{(\ell+\rho_1)(\ell+\sigma_1)(2\ell+\rho_1+\sigma_1+2)}{(\ell+1)(\ell+\rho_1+\sigma_1+1)(2\ell+\rho_1+\sigma_1)}.\end{cases} \tag{13}$$

Theorem 2.3 The R-JPs satisfy [35]

$$\varrho(\varrho+1)\partial_\varrho\hat{\mathcal{R}}_\ell^{\rho_1,\sigma_1}(\varrho) = A_\ell^{\rho_1,\sigma_1}\hat{\mathcal{R}}_{\ell-1}^{\rho_1,\sigma_1}(\varrho) + B_\ell^{\rho_1,\sigma_1}\hat{\mathcal{R}}_\ell^{\rho_1,\sigma_1}(\varrho) + C_\ell^{\rho_1,\sigma_1}\hat{\mathcal{R}}_{\ell+1}^{\rho_1,\sigma_1}(\varrho), \tag{14}$$

where

$$\begin{aligned} A_{\ell}^{\rho_1,\sigma_1} &= -\frac{(\ell+\rho_1)(\ell+\sigma_1)(\ell+\rho_1+\sigma_1+1)}{(2\ell+\rho_1+\sigma_1+1)(2\ell+\rho_1+\sigma_1)}, \\ B_{\ell}^{\rho_1,\sigma_1} &= \frac{\ell(\sigma_1-\rho_1)(\ell+\rho_1+\sigma_1+1)}{(2\ell+\rho_1+\sigma_1)(2\ell+\rho_1+\sigma_1+2)}, \\ C_{\ell}^{\rho_1,\sigma_1} &= \frac{\ell(\ell+1)(\ell+\rho_1+\sigma_1+1)}{(2\ell+\rho_1+\sigma_1+1)(2\ell+\rho_1+\sigma_1+2)}. \end{aligned} \tag{15}$$

Lemma 2.4 The R-JPs are the eigenfunctions of the singular Sturm–Liouville issue:

$$\mathcal{L}_{\rho_1,\sigma_1}\hat{\mathcal{R}}_{\ell}^{\rho_1,\sigma_1}(\varrho) = \delta_{\ell}^{\rho_1,\sigma_1}\hat{\mathcal{R}}_{\ell}^{\rho_1,\sigma_1}(\varrho), \tag{16}$$

with their corresponding eigenvalues

$$\delta_{\ell}^{\rho_1,\sigma_1} = \ell(\ell+\rho_1+\sigma_1+1) < 0. \tag{17}$$

Theorem 2.5 The R-JP derivatives are provided by [35]

$$\frac{d^q}{d\varrho^q}\hat{\mathcal{R}}_{m}^{\rho_1,\sigma_1}(\varrho) = \sum_{l=0}^{m-q} C_{l,m}^{\rho_1,\sigma_1,q}\hat{\mathcal{R}}_{l}^{\rho_1,\sigma_1}(\varrho), \tag{18}$$

where

$$C_{l,m}^{\rho_1,\sigma_1,q} = \frac{(-1)^q\Gamma(-m-\rho_1-\sigma_1)}{\Gamma(-m-\rho_1-\sigma_1-q)}c_k^{n-q}(\rho_1+q,\sigma_1+q,\rho_1,\sigma_1), \tag{19}$$

Theorem 2.6 (R-J-Gauss quadrature). R-J-Gauss nodes $\{\varrho_\ell\}_{\ell=0}^{M}$ being the zeros of $\hat{\mathcal{R}}_{M+1}^{\rho_1,\sigma_1}$ and the corresponding weights are given by

$$\begin{aligned} \varpi_{\ell}^{\rho_1,\sigma_1} &= \frac{G_M^{\rho_1,\sigma_1}}{\hat{\mathcal{R}}_M^{\rho_1,\sigma_1}(\varrho_\ell)\partial_\varrho\hat{\mathcal{R}}_{M+1}^{\rho_1,\sigma_1}(\varrho_\ell)} \\ &= \frac{\tilde{G}_M^{\rho_1,\sigma_1}}{\varrho_\ell(1+\varrho_\ell)\left[\partial_\varrho\hat{\mathcal{R}}_{M+1}^{\rho_1,\sigma_1}(\varrho_\ell)\right]^2}, \end{aligned} \tag{20}$$

where

$$\begin{aligned} G_M^{\rho_1,\sigma_1} &= \frac{(2M+\rho_1+\sigma_1+2)\Gamma(-M-\rho_1-\sigma_1-1)\Gamma(1+M+\rho_1)}{(M+1)!\Gamma(-M-\sigma_1)}, \\ \tilde{G}_M^{\rho_1,\sigma_1} &= \frac{\Gamma(-M-\rho_1-\sigma_1-1)\Gamma(2+M+\rho_1)}{(M+1)!\Gamma(-M-\sigma_1-1)}. \end{aligned} \tag{21}$$

3. ONE-DIMENSIONAL NONLINEAR DOFCDES

In this Section, we propose a Romanovski–Jacobi spectral collocation (RJSC) method for the numerical solution of non-linear distributed-order fractional convection-

diffusion equations (DOFCDEs). The proposed method is developed as follows:

$$\int_0^1 \aleph(\omega)\, {}^cD_{\varrho}^{\omega}\varphi(\chi,\varrho)\, d\omega + \frac{\partial^2\varphi(\chi,\varrho)}{\partial\chi^2} + \frac{\partial\varphi(\chi,\varrho)}{\partial\chi} = \mathcal{F}(\chi,\varrho,\varphi(\chi,\varrho)), \quad \text{where} \quad \chi\in[0,\zeta], \varrho\in[0,T], \tag{22}$$

with the initial-boundary conditions

$$\varphi(0,\varrho)=\psi_1(\varrho),\ \varphi(\zeta,\varrho)=\psi_2(\varrho),\ \varphi(\chi,0)=\psi_3(\chi). \tag{23}$$

The approximate solution $\breve{\varphi}(\chi,\varrho)$ is constructed by incorporating a spectral expansion based on shifted Jacobi polynomials in conjunction with shifted Romanovski–Jacobi polynomials (R-JPs)

$$\breve{\varphi}(\chi,\varrho) = \sum_{\substack{\hat{s}=0,1,\ldots,\mathcal{M}\\ \hat{\varrho}=0,1,\ldots,\mathcal{N}}} \epsilon_{\hat{s},\hat{\varrho}}\hat{\mathcal{J}}_{\hat{s}}^{\alpha_1,\beta_1}(\chi)\hat{\mathcal{R}}_{\hat{\varrho}}^{\rho_1,\sigma_1,\epsilon}(\varrho), \tag{24}$$

while $\hat{\mathcal{J}}_{\hat{s}}^{\alpha_1,\beta_1}(\chi)$ is shifted Jacobi polynomials $\hat{\mathcal{R}}_{\hat{\varrho}}^{\rho_1,\sigma_1,\epsilon}(\varrho)=\hat{\mathcal{R}}_{\hat{\varrho}}^{\rho_1,\sigma_1}((\varrho)^{\epsilon})$ is fractional R-JPs, and ϵ is a fractional number.
Next, the time derivatives are obtained as

$$\begin{aligned}\frac{\partial\breve{\varphi}}{\partial\varrho} &= \sum_{\substack{\hat{s}=0,1,\ldots,\mathcal{M}\\ \hat{\varrho}=0,1,\ldots,\mathcal{N}}} \epsilon_{\hat{s},\hat{\varrho}}\hat{\mathcal{J}}_{\hat{s}}^{\alpha_1,\beta_1}(\chi)\hat{\mathcal{R}}_{\hat{\varrho},1}^{\rho_1,\sigma_1,\epsilon}(\varrho),\\ \frac{\partial^2\breve{\varphi}}{\partial\varrho^2} &= \sum_{\substack{\hat{s}=0,1,\ldots,\mathcal{M}\\ \hat{\varrho}=0,1,\ldots,\mathcal{N}}} \epsilon_{\hat{s},\hat{\varrho}}\hat{\mathcal{J}}_{\hat{s}}^{\alpha_1,\beta_1}(\chi)\hat{\mathcal{R}}_{\hat{\varrho},2}^{\rho_1,\sigma_1,\epsilon}(\varrho).\end{aligned} \tag{25}$$

Furthermore, the spatial derivatives are

$$\begin{aligned}\frac{\partial\breve{\varphi}}{\partial\chi} &= \sum_{\substack{\hat{s}=0,1,\ldots,\mathcal{M}\\ \hat{\varrho}=0,1,\ldots,\mathcal{N}}} \epsilon_{\hat{s},\hat{\varrho}}\hat{\mathcal{J}}_{\hat{s},1}^{\alpha_1,\beta_1}(\chi)\hat{\mathcal{R}}_{\hat{\varrho}}^{\rho_1,\sigma_1,\epsilon}(\varrho),\\ \frac{\partial^2\breve{\varphi}}{\partial\chi^2} &= \sum_{\substack{\hat{s}=0,1,\ldots,\mathcal{M}\\ \hat{\varrho}=0,1,\ldots,\mathcal{N}}} \epsilon_{\hat{s},\hat{\varrho}}\hat{\mathcal{J}}_{\hat{s},2}^{\alpha_1,\beta_1}(\chi)\hat{\mathcal{R}}_{\hat{\varrho}}^{\rho_1,\sigma_1,\epsilon}(\varrho).\end{aligned} \tag{26}$$

Additionally, ${}^cD_{\varrho}^{\omega}\breve{\varphi}(\chi,\varrho)$, has been provided by

$$\begin{aligned}{}^cD_{\varrho}^{\omega}\breve{\varphi}(\chi,\varrho) &= \sum_{\substack{\hat{s}=0,1,\ldots,\mathcal{M}\\ \hat{\varrho}=0,1,\ldots,\mathcal{N}}} \epsilon_{\hat{s},\hat{\varrho}}\hat{\mathcal{J}}_{\hat{s}}^{\alpha_1,\beta_1}(\chi)\,{}^cD_{\varrho}^{\omega}(\hat{\mathcal{R}}_{\hat{\varrho}}^{\rho_1,\sigma_1,\epsilon}(\varrho))\\ &= \sum_{\substack{\hat{s}=0,1,\ldots,\mathcal{M}\\ \hat{\varrho}=0,1,\ldots,\mathcal{N}}} \epsilon_{\hat{s},\hat{\varrho}}\hat{\mathcal{J}}_{\hat{s}}^{\alpha_1,\beta_1}(\chi)\hat{\mathcal{R}}_{\hat{\varrho},\omega}^{\rho_1,\sigma_1,\epsilon}(\varrho).\end{aligned} \tag{27}$$

We treat the distributed fractional term utilizing shifted Legendre Gauss-Lobatto quadrature as follows:

$$\begin{aligned}\int_0^1 \aleph(\omega)\,{}^cD_{\varrho}^{\omega}\breve{\varphi}(\chi,\varrho)\,d\omega &= \int_0^1 \aleph(\omega) \sum_{\substack{\hat{s}=0,1,\ldots,\mathcal{M}\\ \hat{\varrho}=0,1,\ldots,\mathcal{N}}} \epsilon_{\hat{s},\hat{\varrho}}\hat{\mathcal{J}}_{\hat{s}}^{\alpha_1,\beta_1}(\chi)\hat{\mathcal{R}}_{\hat{\varrho},\omega}^{\rho_1,\sigma_1,\epsilon}(\varrho)d\omega \\ &= \sum_{\substack{\hat{s}=0,1,\ldots,\mathcal{M}\\ \hat{\varrho}=0,1,\ldots,\mathcal{N}}} \epsilon_{\hat{s},\hat{\varrho}}\hat{\mathcal{J}}_{\hat{s}}^{\alpha_1,\beta_1}(\chi)\int_0^1 \aleph(\omega)\hat{\mathcal{R}}_{\hat{\varrho},\omega}^{\rho_1,\sigma_1,\epsilon}(\varrho)d\omega \\ &= \sum_{\substack{\hat{s}=0,1,\ldots,\mathcal{M}\\ \hat{\varrho}=0,1,\ldots,\mathcal{N}}} \epsilon_{\hat{s},\hat{\varrho}}\hat{\mathcal{J}}_{\hat{s}}^{\alpha_1,\beta_1}(\chi)\,{}_0\mathcal{E}_{\hat{\varrho}}^{\rho_1,\sigma_1,\epsilon}(\varrho),\end{aligned} \tag{28}$$

while

$$\begin{aligned}\mathcal{E}_{\hat{\varrho}}^{\rho_1,\sigma_1,\epsilon}(\varrho) &= \int_0^1 \aleph(\omega)\hat{\mathcal{R}}_{\hat{\varrho},\omega}^{\rho_1,\sigma_1,\epsilon}(\varrho)d\omega \\ &= \sum_{\hat{w}=0,1,\ldots,\mathcal{W}} {}_0\mathbf{W}_1^{\mathcal{W},\hat{w}}\aleph({}_0\Omega_1^{\hat{w}})\hat{\mathcal{R}}_{\hat{\varrho},{}_0\Omega_1^{\hat{w}}}^{\rho_1,\sigma_1,\epsilon}(\varrho).\end{aligned}$$

Combing Eqs. (22)-(28), we obtain

$$\begin{aligned}&\sum_{\substack{\hat{s}=0,1,\ldots,\mathcal{M}\\ \hat{\varrho}=0,1,\ldots,\mathcal{N}}} \epsilon_{\hat{s},\hat{\varrho}}\hat{\mathcal{J}}_{\hat{s}}^{\alpha_1,\beta_1}(\chi)\,{}_0\mathcal{E}_{\hat{\varrho}}^{\rho_1,\sigma_1,\epsilon}(\varrho) + \sum_{\substack{\hat{s}=0,1,\ldots,\mathcal{M}\\ \hat{\varrho}=0,1,\ldots,\mathcal{N}}} \epsilon_{\hat{s},\hat{\varrho}}\hat{\mathcal{J}}_{\hat{s},2}^{\alpha_1,\beta_1}(\chi)\hat{\mathcal{R}}_{\hat{\varrho}}^{\rho_1,\sigma_1,\epsilon}(\varrho) \\ &+ \sum_{\substack{\hat{s}=0,1,\ldots,\mathcal{M}\\ \hat{\varrho}=0,1,\ldots,\mathcal{N}}} \epsilon_{\hat{s},\hat{\varrho}}\hat{\mathcal{J}}_{\hat{s},1}^{\alpha_1,\beta_1}(\chi)\hat{\mathcal{R}}_{\hat{\varrho}}^{\rho_1,\sigma_1,\epsilon}(\varrho) = \mathcal{F}(\chi,\varrho,\sum_{\substack{\hat{s}=0,1,\ldots,\mathcal{M}\\ \hat{\varrho}=0,1,\ldots,\mathcal{N}}} \epsilon_{\hat{s},\hat{\varrho}}\hat{\mathcal{J}}_{\hat{s}}^{\alpha_1,\beta_1}(\chi)\hat{\mathcal{R}}_{\hat{\varrho}}^{\rho_1,\sigma_1,\epsilon}(\varrho)).\end{aligned} \tag{29}$$

Furthermore, the given conditions can be expressed as

$$\begin{cases} \sum\limits_{\substack{\hat{s}=0,1,\ldots,\mathcal{M}\\ \hat{\varrho}=0,1,\ldots,\mathcal{N}}} \epsilon_{\hat{s},\hat{\varrho}}\hat{\mathcal{J}}_{\hat{s}}^{\alpha_1,\beta_1}(0)\hat{\mathcal{R}}_{\hat{\varrho}}^{\rho_1,\sigma_1,\epsilon}(\varrho) = \psi_1(\varrho), \\ \sum\limits_{\substack{\hat{s}=0,1,\ldots,\mathcal{M}\\ \hat{\varrho}=0,1,\ldots,\mathcal{N}}} \epsilon_{\hat{s},\hat{\varrho}}\hat{\mathcal{J}}_{\hat{s}}^{\alpha_1,\beta_1}(\zeta)\hat{\mathcal{R}}_{\hat{\varrho}}^{\rho_1,\sigma_1,\epsilon}(\varrho) = \psi_2(\varrho), \\ \sum\limits_{\substack{\hat{s}=0,1,\ldots,\mathcal{M}\\ \hat{\varrho}=0,1,\ldots,\mathcal{N}}} \epsilon_{\hat{s},\hat{\varrho}}\hat{\mathcal{J}}_{\hat{s}}^{\alpha_1,\beta_1}(\chi)\hat{\mathcal{R}}_{\hat{\varrho}}^{\rho_1,\sigma_1,\epsilon}(0) = \psi_3(\chi). \end{cases} \tag{30}$$

The equations (29) and (30) are nearest to being zero at specific nodes:

$$\begin{cases} \sum_{\substack{\hat{s}=0,1,\ldots,\mathcal{M}\\ \hat{\varrho}=0,1,\ldots,\mathcal{N}}} \epsilon_{\hat{s},\hat{\varrho}} \hat{\mathcal{J}}_{\hat{s}}^{\alpha_1,\beta_1}(\chi_{\mathcal{M},\iota}^{\alpha_1,\beta_1})\, {}_0\mathcal{E}_{\hat{\varrho}}^{\rho_1,\sigma_1,\epsilon}(\varrho_\kappa^{\rho_1,\sigma_1,\epsilon}) \\ + \sum_{\substack{\hat{s}=0,1,\ldots,\mathcal{M}\\ \hat{\varrho}=0,1,\ldots,\mathcal{N}}} \epsilon_{\hat{s},\hat{\varrho}} \hat{\mathcal{J}}_{\hat{s},2}^{\alpha_1,\beta_1}(\chi_{\mathcal{M},\iota}^{\alpha_1,\beta_1}) \hat{\mathcal{R}}_{\hat{\varrho}}^{\rho_1,\sigma_1,\epsilon}(\varrho_\kappa^{\rho_1,\sigma_1,\epsilon}) \\ + \sum_{\substack{\hat{s}=0,1,\ldots,\mathcal{M}\\ \hat{\varrho}=0,1,\ldots,\mathcal{N}}} \epsilon_{\hat{s},\hat{\varrho}} \hat{\mathcal{J}}_{\hat{s},1}^{\alpha_1,\beta_1}(\chi_{\mathcal{M},\iota}^{\alpha_1,\beta_1}) \hat{\mathcal{R}}_{\hat{\varrho}}^{\rho_1,\sigma_1,\epsilon}(\varrho_\kappa^{\rho_1,\sigma_1,\epsilon}) \\ = \mathcal{F}\left(\chi_{\mathcal{M},\iota}^{\alpha_1,\beta_1}, \varrho_\kappa^{\rho_1,\sigma_1,\epsilon}, \sum_{\substack{\hat{s}=0,1,\ldots,\mathcal{M}\\ \hat{\varrho}=0,1,\ldots,\mathcal{N}}} \epsilon_{\hat{s},\hat{\varrho}} \hat{\mathcal{J}}_{\hat{s}}^{\alpha_1,\beta_1}(\chi_{\mathcal{M},\iota}^{\alpha_1,\beta_1}) \hat{\mathcal{R}}_{\hat{\varrho}}^{\rho_1,\sigma_1,\epsilon}(\varrho_\kappa^{\rho_1,\sigma_1,\epsilon}) \right), \\ \sum_{\substack{\hat{s}=0,1,\ldots,\mathcal{M}\\ \hat{\varrho}=0,1,\ldots,\mathcal{N}}} \epsilon_{\hat{s},\hat{\varrho}} \hat{\mathcal{J}}_{\hat{s}}^{\alpha_1,\beta_1}(0) \hat{\mathcal{R}}_{\hat{\varrho}}^{\rho_1,\sigma_1,\epsilon}(\varrho_\kappa^{\rho_1,\sigma_1,\epsilon}) = \psi_1(\varrho_\kappa^{\rho_1,\sigma_1,\epsilon}), \\ \sum_{\substack{\hat{s}=0,1,\ldots,\mathcal{M}\\ \hat{\varrho}=0,1,\ldots,\mathcal{N}}} \epsilon_{\hat{s},\hat{\varrho}} \hat{\mathcal{J}}_{\hat{s}}^{\alpha_1,\beta_1}(\zeta) \hat{\mathcal{R}}_{\hat{\varrho}}^{\rho_1,\sigma_1,\epsilon}(\varrho_\kappa^{\rho_1,\sigma_1,\epsilon}) = \psi_2(\varrho_\kappa^{\rho_1,\sigma_1,\epsilon}), \\ \sum_{\substack{\hat{s}=0,1,\ldots,\mathcal{M}\\ \hat{\varrho}=0,1,\ldots,\mathcal{N}}} \epsilon_{\hat{s},\hat{\varrho}} \hat{\mathcal{J}}_{\hat{s}}^{\alpha_1,\beta_1}(\chi_{\mathcal{M},\iota}^{\alpha_1,\beta_1}) \hat{\mathcal{R}}_{\hat{\varrho}}^{\rho_1,\sigma_1,\epsilon}(0) = \psi_3(\chi_{\mathcal{M},\iota}^{\alpha_1,\beta_1}). \end{cases} \tag{31}$$

Finally, the resulting system can be solved in a straightforward manner, yielding a closed-form expression for the approximate solution $\breve{\varphi}(\chi,\varrho)$.

4. TWO-DIMENSIONAL NONLINEAR DOFCDES

In this Section, we present a numerical technique for solving the 2D nonlinear distributed-order fractional convection-diffusion equation (2D-DOFCDEs) using RJSC method.

$$\begin{aligned} \int_0^1 \aleph(\omega)\, {}^cD_\varrho^\omega \varphi(\chi,\varrho,\xi)\, d\omega + \frac{\partial^2\varphi(\chi,\varrho,\xi)}{\partial\chi^2} + \frac{\partial^2\varphi(\chi,\varrho,\xi)}{\partial\varrho^2} + \frac{\partial\varphi(\chi,\varrho,\xi)}{\partial\chi} + \frac{\partial\varphi(\chi,\varrho,\xi)}{\partial\varrho} \\ = \mathcal{F}(\chi,\varrho,\xi,\varphi(\chi,\varrho,\xi)), \qquad \text{where} \quad \chi\in[0,\zeta_1], \varrho\in[0,\zeta_2], \xi\in[0,T], \end{aligned} \tag{32}$$

with the initial-boundary conditions

$$\begin{cases} \varphi(0,\varrho,\xi) = \psi_1(\varrho,\xi), \\ \varphi(\zeta_1,\varrho,\xi) = \psi_2(\varrho,\xi), \\ \varphi(\chi,0,\xi) = \psi_3(\chi,\xi), \\ \varphi(\chi,\zeta_2,\xi) = \psi_4(\chi,\xi), \\ \varphi(\chi,\varrho,0) = \psi_5(\chi,\varrho). \end{cases} \tag{33}$$

Here the functions $\psi_1(\varrho,\xi)$, $\psi_2(\varrho,\xi)$, $\psi_3(\chi,\xi)$, $\psi_4(\chi,\xi)$, and $\psi_5(\chi,\varrho)$ are known.

The approximate solution $\breve{\varphi}(\chi,\varrho,\xi)$ is constructed by incorporating a spectral expansion based on shifted Jacobi functions in conjunction with shifted Romanovski–

Jacobi polynomials (R-JPs).

$$\breve{\varphi}(\chi,\varrho,\xi)=\sum_{\substack{\hat{s}=0,1,...,\mathcal{M}\\ \hat{\varrho}=0,1,...,\mathcal{N}\\ \hat{v}=0,1,...,\mathcal{K}}}\epsilon_{\hat{s},\hat{\varrho},\hat{v}}\hat{\mathcal{J}}_{\hat{s}}^{\alpha_1,\beta_1}(\chi)\hat{\mathcal{J}}_{\hat{\varrho}}^{\alpha_2,\beta_2}(\varrho)\hat{\mathcal{R}}_{\hat{v}}^{\rho_1,\sigma_1,\epsilon}(\xi), \tag{34}$$

while $\hat{\mathcal{J}}_{\hat{s}}^{\alpha_j,\beta}(\chi)$ for $j=1,2$ represent shifted Jacobi polynomials and the third basis $\hat{\mathcal{R}}_{\hat{\varrho}}^{\rho_1,\sigma_1,\epsilon}(\varrho)=\hat{\mathcal{R}}_{\hat{\varrho}}^{\rho_1,\sigma_1}((\varrho)^{\epsilon})$ is fractional R-JPs, and ϵ is a fractional number.

Let us calculate the integer-order spatial derivatives of

$$\begin{aligned}\frac{\partial\breve{\varphi}}{\partial\chi}&=\sum_{\substack{\hat{s}=0,1,...,\mathcal{M}\\ \hat{\varrho}=0,1,...,\mathcal{N}\\ \hat{v}=0,1,...,\mathcal{K}}}\epsilon_{\hat{s},\hat{\varrho},\hat{v}}\hat{\mathcal{J}}_{\hat{s},1}^{\alpha_1,\beta_1}(\chi)\hat{\mathcal{J}}_{\hat{\varrho}}^{\alpha_2,\beta_2}(\varrho)\hat{\mathcal{R}}_{\hat{v}}^{\rho_1,\sigma_1,\epsilon}(\xi),\\ \frac{\partial^2\breve{\varphi}}{\partial\chi^2}&=\sum_{\substack{\hat{s}=0,1,...,\mathcal{M}\\ \hat{\varrho}=0,1,...,\mathcal{N}\\ \hat{v}=0,1,...,\mathcal{K}}}\epsilon_{\hat{s},\hat{\varrho},\hat{v}}\hat{\mathcal{J}}_{\hat{s},2}^{\alpha_1,\beta_1}(\chi)\hat{\mathcal{J}}_{\hat{\varrho}}^{\alpha_2,\beta_2}(\varrho)\hat{\mathcal{R}}_{\hat{v}}^{\rho_1,\sigma_1,\epsilon}(\xi).\end{aligned} \tag{35}$$

$$\frac{\partial\breve{\varphi}}{\partial\chi}+\frac{\partial^2\breve{\varphi}}{\partial\chi^2}=\sum_{\substack{\hat{s}=0,1,...,\mathcal{M}\\ \hat{\varrho}=0,1,...,\mathcal{N}\\ \hat{v}=0,1,...,\mathcal{K}}}\epsilon_{\hat{s},\hat{\varrho},\hat{v}}\left(\hat{\mathcal{J}}_{\hat{s},1}^{\alpha_1,\beta_1}(\chi)+\hat{\mathcal{J}}_{\hat{s},2}^{\alpha_1,\beta_1}(\chi)\right)\hat{\mathcal{J}}_{\hat{\varrho}}^{\alpha_2,\beta_2}(\varrho)\hat{\mathcal{R}}_{\hat{v}}^{\rho_1,\sigma_1,\epsilon}(\xi). \tag{36}$$

Also

$$\begin{aligned}\frac{\partial\breve{\varphi}}{\partial\varrho}&=\sum_{\substack{\hat{s}=0,1,...,\mathcal{M}\\ \hat{\varrho}=0,1,...,\mathcal{N}\\ \hat{v}=0,1,...,\mathcal{K}}}\epsilon_{\hat{s},\hat{\varrho},\hat{v}}\hat{\mathcal{J}}_{\hat{s}}^{\alpha_1,\beta_1}(\chi)\hat{\mathcal{J}}_{\hat{\varrho},1}^{\alpha_2,\beta_2}(\varrho)\hat{\mathcal{R}}_{\hat{v}}^{\rho_1,\sigma_1,\epsilon}(\xi),\\ \frac{\partial^2\breve{\varphi}}{\partial\varrho^2}&=\sum_{\substack{\hat{s}=0,1,...,\mathcal{M}\\ \hat{\varrho}=0,1,...,\mathcal{N}\\ \hat{v}=0,1,...,\mathcal{K}}}\epsilon_{\hat{s},\hat{\varrho},\hat{v}}\hat{\mathcal{J}}_{\hat{s}}^{\alpha_1,\beta_1}(\chi)\hat{\mathcal{J}}_{\hat{\varrho},2}^{\alpha_2,\beta_2}(\varrho)\hat{\mathcal{R}}_{\hat{v}}^{\rho_1,\sigma_1,\epsilon}(\xi).\end{aligned} \tag{37}$$

$$\frac{\partial\breve{\varphi}}{\partial\varrho}+\frac{\partial^2\breve{\varphi}}{\partial\varrho^2}=\sum_{\substack{\hat{s}=0,1,...,\mathcal{M}\\ \hat{\varrho}=0,1,...,\mathcal{N}\\ \hat{v}=0,1,...,\mathcal{K}}}\epsilon_{\hat{s},\hat{\varrho},\hat{v}}\hat{\mathcal{J}}_{\hat{s}}^{\alpha_1,\beta_1}(\chi)\left(\hat{\mathcal{J}}_{\hat{\varrho},1}^{\alpha_2,\beta_2}(\varrho)+\hat{\mathcal{J}}_{\hat{\varrho},2}^{\alpha_2,\beta_2}(\varrho)\right)\hat{\mathcal{R}}_{\hat{v}}^{\rho_1,\sigma_1,\epsilon}(\xi). \tag{38}$$

Additionally, ${}^{c}D_{\varrho}^{\omega}\breve{\varphi}(\chi,\varrho,\xi)$, has been provided by

$$\begin{aligned} {}^{c}D_{\varrho}^{\omega}\breve{\varphi}(\chi,\varrho,\xi) &= \sum_{\substack{\hat{s}=0,1,\ldots,\mathcal{M}\\ \hat{\varrho}=0,1,\ldots,\mathcal{N}\\ \hat{v}=0,1,\ldots,\mathcal{K}}} \epsilon_{\hat{s},\hat{\varrho},\hat{v}}\hat{\mathcal{J}}_{\hat{s}}^{\alpha_1,\beta_1}(\chi)\hat{\mathcal{J}}_{\hat{\varrho}}^{\alpha_2,\beta_2}(\varrho)\,{}^{c}D_{\varrho}^{\omega}(\hat{\mathcal{R}}_{\hat{v}}^{\rho_1,\sigma_1,\epsilon}(\xi)) \\ &= \sum_{\substack{\hat{s}=0,1,\ldots,\mathcal{M}\\ \hat{\varrho}=0,1,\ldots,\mathcal{N}\\ \hat{v}=0,1,\ldots,\mathcal{K}}} \epsilon_{\hat{s},\hat{\varrho},\hat{v}}\hat{\mathcal{J}}_{\hat{s}}^{\alpha_1,\beta_1}(\chi)\hat{\mathcal{J}}_{\hat{\varrho}}^{\alpha_2,\beta_2}(\varrho)\hat{\mathcal{R}}_{\hat{v},\omega}^{\rho_1,\sigma_1,\epsilon}(\xi). \end{aligned} \tag{39}$$

We treat the distributed fractional term utilizing shifted Legendre Gauss–Lobatto quadrature as follows:

$$\begin{aligned} \int_0^1 \aleph(\omega)\,{}^{c}D_{\varrho}^{\omega}\breve{\varphi}(\chi,\varrho,\xi)\,d\omega &= \int_0^1 \aleph(\omega) \sum_{\substack{\hat{s}=0,1,\ldots,\mathcal{M}\\ \hat{\varrho}=0,1,\ldots,\mathcal{N}\\ \hat{v}=0,1,\ldots,\mathcal{K}}} \epsilon_{\hat{s},\hat{\varrho},\hat{v}}\hat{\mathcal{J}}_{\hat{s}}^{\alpha_1,\beta_1}(\chi)\hat{\mathcal{J}}_{\hat{\varrho}}^{\alpha_2,\beta_2}(\varrho)\hat{\mathcal{R}}_{\hat{v},\omega}^{\rho_1,\sigma_1,\epsilon}(\xi)d\omega \\ &= \sum_{\substack{\hat{s}=0,1,\ldots,\mathcal{M}\\ \hat{\varrho}=0,1,\ldots,\mathcal{N}\\ \hat{v}=0,1,\ldots,\mathcal{K}}} \epsilon_{\hat{s},\hat{\varrho},\hat{v}}\hat{\mathcal{J}}_{\hat{s}}^{\alpha_1,\beta_1}(\chi)\hat{\mathcal{J}}_{\hat{\varrho}}^{\alpha_2,\beta_2}(\varrho)\int_0^1 \aleph(\omega)\hat{\mathcal{R}}_{\hat{v},\omega}^{\rho_1,\sigma_1,\epsilon}(\xi)d\omega \\ &= \sum_{\substack{\hat{s}=0,1,\ldots,\mathcal{M}\\ \hat{\varrho}=0,1,\ldots,\mathcal{N}\\ \hat{v}=0,1,\ldots,\mathcal{K}}} \epsilon_{\hat{s},\hat{\varrho},\hat{v}}\hat{\mathcal{J}}_{\hat{s}}^{\alpha_1,\beta_1}(\chi)\hat{\mathcal{J}}_{\hat{\varrho}}^{\alpha_2,\beta_2}(\varrho)\hat{\mathcal{Q}}_{\hat{v}}^{\rho_1,\sigma_1,\epsilon}(\xi), \end{aligned} \tag{40}$$

where

$$\begin{aligned} \hat{\mathcal{Q}}_{\hat{v}}^{\rho_1,\sigma_1,\epsilon}(\xi) &= \int_0^1 \aleph(\omega)\hat{\mathcal{R}}_{\hat{s},\omega}^{\rho_1,\sigma_1,\epsilon}(\xi)d\omega \\ &= \sum_{\hat{w}=0,1,\ldots,\mathcal{W}} {}_0\mathbf{W}_1^{\mathcal{W},\hat{w}}\aleph({}_0\Omega_1^{\hat{w}})\hat{\mathcal{R}}_{\hat{s},{}_0\Omega_1^{\hat{w}}}^{\rho_1,\sigma_1,\epsilon}(\xi). \end{aligned}$$

Combing Eqs. (32)-(40), we obtain

$$\begin{aligned}
&\sum_{\substack{\hat{s}=0,1,\ldots,\mathcal{M}\\ \hat{\varrho}=0,1,\ldots,\mathcal{N}\\ \hat{v}=0,1,\ldots,\mathcal{K}}} \epsilon_{\hat{s},\hat{\varrho},\hat{v}} \hat{\mathcal{J}}_{\hat{s}}^{\alpha_1,\beta_1}(\chi)\hat{\mathcal{J}}_{\hat{\varrho}}^{\alpha_2,\beta_2}(\varrho)\hat{\mathcal{Q}}_{\hat{v}}^{\rho_1,\sigma_1,\epsilon}(\xi)\\
&+\sum_{\substack{\hat{s}=0,1,\ldots,\mathcal{M}\\ \hat{\varrho}=0,1,\ldots,\mathcal{N}\\ \hat{v}=0,1,\ldots,\mathcal{K}}} \epsilon_{\hat{s},\hat{\varrho},\hat{v}} \left(\hat{\mathcal{J}}_{\hat{s},1}^{\alpha_1,\beta_1}(\chi)+\hat{\mathcal{J}}_{\hat{s},2}^{\alpha_1,\beta_1}(\chi)\right)\hat{\mathcal{J}}_{\hat{\varrho}}^{\alpha_2,\beta_2}(\varrho)\hat{\mathcal{R}}_{\hat{v}}^{\rho_1,\sigma_1,\epsilon}(\xi)\\
&+\sum_{\substack{\hat{s}=0,1,\ldots,\mathcal{M}\\ \hat{\varrho}=0,1,\ldots,\mathcal{N}\\ \hat{v}=0,1,\ldots,\mathcal{K}}} \epsilon_{\hat{s},\hat{\varrho},\hat{v}} \hat{\mathcal{J}}_{\hat{s}}^{\alpha_1,\beta_1}(\chi)\left(\hat{\mathcal{J}}_{\hat{\varrho},1}^{\alpha_2,\beta_2}(\varrho)+\hat{\mathcal{J}}_{\hat{\varrho},2}^{\alpha_2,\beta_2}(\varrho)\right)\hat{\mathcal{R}}_{\hat{v}}^{\rho_1,\sigma_1,\epsilon}(\xi)\\
=&\mathcal{F}\Big(\chi,\varrho,\xi,\sum_{\substack{\hat{s}=0,1,\ldots,\mathcal{M}\\ \hat{\varrho}=0,1,\ldots,\mathcal{N}\\ \hat{v}=0,1,\ldots,\mathcal{K}}} \epsilon_{\hat{s},\hat{\varrho},\hat{v}} \hat{\mathcal{J}}_{\hat{s}}^{\alpha_1,\beta_1}(\chi)\hat{\mathcal{J}}_{\hat{\varrho}}^{\alpha_2,\beta_2}(\varrho)\hat{\mathcal{R}}_{\hat{v}}^{\rho_1,\sigma_1,\epsilon}(\xi)\Big).
\end{aligned} \tag{41}$$

Furthermore, the given conditions can be expressed as

$$\begin{cases}
\sum_{\substack{\hat{s}=0,1,\ldots,\mathcal{M}\\ \hat{\varrho}=0,1,\ldots,\mathcal{N}\\ \hat{v}=0,1,\ldots,\mathcal{K}}} \epsilon_{\hat{s},\hat{\varrho},\hat{v}} \hat{\mathcal{J}}_{\hat{s}}^{\alpha_1,\beta_1}(0)\hat{\mathcal{J}}_{\hat{\varrho}}^{\alpha_2,\beta_2}(\varrho)\hat{\mathcal{R}}_{\hat{v}}^{\rho_1,\sigma_1,\epsilon}(\xi)=\psi_1(\varrho,\xi),\\
\sum_{\substack{\hat{s}=0,1,\ldots,\mathcal{M}\\ \hat{\varrho}=0,1,\ldots,\mathcal{N}\\ \hat{v}=0,1,\ldots,\mathcal{K}}} \epsilon_{\hat{s},\hat{\varrho},\hat{v}} \hat{\mathcal{J}}_{\hat{s}}^{\alpha_1,\beta_1}(\zeta_1)\hat{\mathcal{J}}_{\hat{\varrho}}^{\alpha_2,\beta_2}(\varrho)\hat{\mathcal{R}}_{\hat{v}}^{\rho_1,\sigma_1,\epsilon}(\xi)=\psi_2(\varrho,\xi),\\
\sum_{\substack{\hat{s}=0,1,\ldots,\mathcal{M}\\ \hat{\varrho}=0,1,\ldots,\mathcal{N}\\ \hat{v}=0,1,\ldots,\mathcal{K}}} \epsilon_{\hat{s},\hat{\varrho},\hat{v}} \hat{\mathcal{J}}_{\hat{s}}^{\alpha_1,\beta_1}(\chi)\hat{\mathcal{J}}_{\hat{\varrho}}^{\alpha_2,\beta_2}(0)\hat{\mathcal{R}}_{\hat{v}}^{\rho_1,\sigma_1,\epsilon}(\xi)=\psi_3(\chi,\xi),\\
\sum_{\substack{\hat{s}=0,1,\ldots,\mathcal{M}\\ \hat{\varrho}=0,1,\ldots,\mathcal{N}\\ \hat{v}=0,1,\ldots,\mathcal{K}}} \epsilon_{\hat{s},\hat{\varrho},\hat{v}} \hat{\mathcal{J}}_{\hat{s}}^{\alpha_1,\beta_1}(\chi)\hat{\mathcal{J}}_{\hat{\varrho}}^{\alpha_2,\beta_2}(\zeta_2)\hat{\mathcal{R}}_{\hat{v}}^{\rho_1,\sigma_1,\epsilon}(\xi)=\psi_4(\chi,\xi),\\
\sum_{\substack{\hat{s}=0,1,\ldots,\mathcal{M}\\ \hat{\varrho}=0,1,\ldots,\mathcal{N}\\ \hat{v}=0,1,\ldots,\mathcal{K}}} \epsilon_{\hat{s},\hat{\varrho},\hat{v}} \hat{\mathcal{J}}_{\hat{s}}^{\alpha_1,\beta_1}(\chi)\hat{\mathcal{J}}_{\hat{\varrho}}^{\alpha_2,\beta_2}(\varrho)\hat{\mathcal{R}}_{\hat{v}}^{\rho_1,\sigma_1,\epsilon}(0)=\psi_5(\chi,\varrho).
\end{cases} \tag{42}$$

The equations (41) and (42) are nearest to being zero at specific nodes:

$$
\begin{cases}
\sum_{\substack{\hat{s}=0,1,\ldots,\mathcal{M}\\ \hat{\varrho}=0,1,\ldots,\mathcal{N}\\ \hat{v}=0,1,\ldots,\mathcal{K}}} \epsilon_{\hat{s},\hat{\varrho},\hat{v}} \hat{\mathcal{J}}_{\hat{s}}^{\alpha_1,\beta_1}(\chi_{\mathcal{M},\iota}^{\alpha_1,\beta_1}) \hat{\mathcal{J}}_{\hat{\varrho}}^{\alpha_2,\beta_2}(\varrho_{\mathcal{N},\jmath}^{\alpha_2,\beta_2}) \hat{\mathcal{Q}}_{\hat{v}}^{\rho_1,\sigma_1,\epsilon}(\xi_\tau^{\rho_1,\sigma_1,\epsilon}) \\
+ \sum_{\substack{\hat{s}=0,1,\ldots,\mathcal{M}\\ \hat{\varrho}=0,1,\ldots,\mathcal{N}\\ \hat{v}=0,1,\ldots,\mathcal{K}}} \epsilon_{\hat{s},\hat{\varrho},\hat{v}} \left(\hat{\mathcal{J}}_{\hat{s},1}^{\alpha_1,\beta_1}(\chi_{\mathcal{M},\iota}^{\alpha_1,\beta_1}) + \hat{\mathcal{J}}_{\hat{s},2}^{\alpha_1,\beta_1}(\chi_{\mathcal{M},\iota}^{\alpha_1,\beta_1}) \right) \hat{\mathcal{J}}_{\hat{\varrho}}^{\alpha_2,\beta_2}(\varrho_{\mathcal{N},\jmath}^{\alpha_2,\beta_2}) \hat{\mathcal{R}}_{\hat{v}}^{\rho_1,\sigma_1,\epsilon}(\xi_\tau^{\rho_1,\sigma_1,\epsilon}) \\
+ \sum_{\substack{\hat{s}=0,1,\ldots,\mathcal{M}\\ \hat{\varrho}=0,1,\ldots,\mathcal{N}\\ \hat{v}=0,1,\ldots,\mathcal{K}}} \epsilon_{\hat{s},\hat{\varrho},\hat{v}} \hat{\mathcal{J}}_{\hat{s}}^{\alpha_1,\beta_1}(\chi_{\mathcal{M},\iota}^{\alpha_1,\beta_1}) \left(\hat{\mathcal{J}}_{\hat{\varrho},1}^{\alpha_2,\beta_2}(\varrho_{\mathcal{N},\jmath}^{\alpha_2,\beta_2}) + \hat{\mathcal{J}}_{\hat{\varrho},2}^{\alpha_2,\beta_2}(\varrho_{\mathcal{N},\jmath}^{\alpha_2,\beta_2}) \right) \hat{\mathcal{R}}_{\hat{v}}^{\rho_1,\sigma_1,\epsilon}(\xi_\tau^{\rho_1,\sigma_1,\epsilon}) \\
= \mathcal{F}(\chi_{\mathcal{M},\iota}^{\alpha_1,\beta_1}, \varrho_{\mathcal{N},\jmath}^{\alpha_2,\beta_2}, \xi_\tau^{\rho_1,\sigma_1,\epsilon}, \sum_{\substack{\hat{s}=0,1,\ldots,\mathcal{M}\\ \hat{\varrho}=0,1,\ldots,\mathcal{N}\\ \hat{v}=0,1,\ldots,\mathcal{K}}} \epsilon_{\hat{s},\hat{\varrho},\hat{v}} \hat{\mathcal{J}}_{\hat{s}}^{\alpha_1,\beta_1}(\chi_{\mathcal{M},\iota}^{\alpha_1,\beta_1}) \hat{\mathcal{J}}_{\hat{\varrho}}^{\alpha_2,\beta_2}(\varrho_{\mathcal{N},\jmath}^{\alpha_2,\beta_2}) \hat{\mathcal{R}}_{\hat{v}}^{\rho_1,\sigma_1,\epsilon}(\xi_\tau^{\rho_1,\sigma_1,\epsilon})), \\
\sum_{\substack{\hat{s}=0,1,\ldots,\mathcal{M}\\ \hat{\varrho}=0,1,\ldots,\mathcal{N}\\ \hat{v}=0,1,\ldots,\mathcal{K}}} \epsilon_{\hat{s},\hat{\varrho},\hat{v}} \hat{\mathcal{J}}_{\hat{s}}^{\alpha_1,\beta_1}(0) \hat{\mathcal{J}}_{\hat{\varrho}}^{\alpha_2,\beta_2}(\varrho_{\mathcal{N},\jmath}^{\alpha_2,\beta_2}) \hat{\mathcal{R}}_{\hat{v}}^{\rho_1,\sigma_1,\epsilon}(\xi_\tau^{\rho_1,\sigma_1,\epsilon}) = \psi_1(\varrho_{\mathcal{N},\jmath}^{\alpha_2,\beta_2}, \xi_\tau^{\rho_1,\sigma_1,\epsilon}), \\
\sum_{\substack{\hat{s}=0,1,\ldots,\mathcal{M}\\ \hat{\varrho}=0,1,\ldots,\mathcal{N}\\ \hat{v}=0,1,\ldots,\mathcal{K}}} \epsilon_{\hat{s},\hat{\varrho},\hat{v}} \hat{\mathcal{J}}_{\hat{s}}^{\alpha_1,\beta_1}(\zeta_1) \hat{\mathcal{J}}_{\hat{\varrho}}^{\alpha_2,\beta_2}(\varrho_{\mathcal{N},\jmath}^{\alpha_2,\beta_2}) \hat{\mathcal{R}}_{\hat{v}}^{\rho_1,\sigma_1,\epsilon}(\xi_\tau^{\rho_1,\sigma_1,\epsilon}) = \psi_2(\varrho_{\mathcal{N},\jmath}^{\alpha_2,\beta_2}, \xi_\tau^{\rho_1,\sigma_1,\epsilon}), \\
\sum_{\substack{\hat{s}=0,1,\ldots,\mathcal{M}\\ \hat{\varrho}=0,1,\ldots,\mathcal{N}\\ \hat{v}=0,1,\ldots,\mathcal{K}}} \epsilon_{\hat{s},\hat{\varrho},\hat{v}} \hat{\mathcal{J}}_{\hat{s}}^{\alpha_1,\beta_1}(\chi_{\mathcal{M},\iota}^{\alpha_1,\beta_1}) \hat{\mathcal{J}}_{\hat{\varrho}}^{\alpha_2,\beta_2}(0) \hat{\mathcal{R}}_{\hat{v}}^{\rho_1,\sigma_1,\epsilon}(\xi_\tau^{\rho_1,\sigma_1,\epsilon}) = \psi_3(\chi_{\mathcal{M},\iota}^{\alpha_1,\beta_1}, \xi_\tau^{\rho_1,\sigma_1,\epsilon}), \\
\sum_{\substack{\hat{s}=0,1,\ldots,\mathcal{M}\\ \hat{\varrho}=0,1,\ldots,\mathcal{N}\\ \hat{v}=0,1,\ldots,\mathcal{K}}} \epsilon_{\hat{s},\hat{\varrho},\hat{v}} \hat{\mathcal{J}}_{\hat{s}}^{\alpha_1,\beta_1}(\chi_{\mathcal{M},\iota}^{\alpha_1,\beta_1}) \hat{\mathcal{J}}_{\hat{\varrho}}^{\alpha_2,\beta_2}(\zeta_2) \hat{\mathcal{R}}_{\hat{v}}^{\rho_1,\sigma_1,\epsilon}(\xi_\tau^{\rho_1,\sigma_1,\epsilon}) = \psi_4(\chi_{\mathcal{M},\iota}^{\alpha_1,\beta_1}, \xi_\tau^{\rho_1,\sigma_1,\epsilon}), \\
\sum_{\substack{\hat{s}=0,1,\ldots,\mathcal{M}\\ \hat{\varrho}=0,1,\ldots,\mathcal{N}\\ \hat{v}=0,1,\ldots,\mathcal{K}}} \epsilon_{\hat{s},\hat{\varrho},\hat{v}} \hat{\mathcal{J}}_{\hat{s}}^{\alpha_1,\beta_1}(\chi_{\mathcal{M},\iota}^{\alpha_1,\beta_1}) \hat{\mathcal{J}}_{\hat{\varrho}}^{\alpha_2,\beta_2}(\varrho_{\mathcal{N},\jmath}^{\alpha_2,\beta_2}) \hat{\mathcal{R}}_{\hat{v}}^{\rho_1,\sigma_1,\epsilon}(0) = \psi_5(\chi_{\mathcal{M},\iota}^{\alpha_1,\beta_1}, \varrho_{\mathcal{N},\jmath}^{\alpha_2,\beta_2}).
\end{cases}
\tag{43}
$$

Finally, the resulting system can be solved in a straightforward manner, yielding a closed-form expression for the approximate solution $\breve{\varphi}(\chi, \varrho, \xi)$.

5. COMPUTATIONAL EVIDENCES

The efficacy and accuracy of the proposed approach are demonstrated through a series of numerical problems. In each case, the absolute error (AE) is computed to quantify the difference between the exact (analytical) solution and the numerically predicted solution:

$$AEs(\chi, \varrho) = |\varphi(\chi, \varrho) - \breve{\varphi}(\chi, \varrho)|, \quad AEs(\chi, \varrho, \xi) = |\varphi(\chi, \varrho, \xi) - \breve{\varphi}(\chi, \varrho, \xi)|. \tag{44}$$

For the point χ, ϱ, ξ, the approximate and exact solutions are $\varphi(\chi, \varrho)$ and $\breve{\varphi}(\chi, \varrho)$. The approach for determining the largest AEs (L_∞) and (L_2) is as described below:

$$L_\infty = \max\{AEs(\chi, \varrho, \xi)\}. \tag{45}$$

Table 1

The MAE for problem 46

$(\mathcal{M},\mathcal{N})$	MAE
$(2,2)$	2.3×10^{-1}
$(4,4)$	6.9×10^{-3}
$(6,6)$	1.7×10^{-5}
$(8,8)$	1.1×10^{-7}
$(10,10)$	4.9×10^{-10}
$(12,12)$	1.6×10^{-12}
$(14,14)$	4.1×10^{-15}

5.1. TEST PROBLEM 1

We consider the non-linear DOFCDEs,

$$\begin{cases} \int_0^1 \aleph(\omega)\, {}^cD_{\varrho}^{\omega}\varphi(\chi,\varrho)\, d\omega - \frac{\partial^2\varphi(\chi,\varrho)}{\partial\chi^2} + \frac{\partial\varphi(\chi,\varrho)}{\partial\chi} + \varphi(\chi,\varrho)^3 = \mathcal{F}(\chi,\varrho), \\ \varphi(0,\varrho) = \psi_1(\varrho), \\ \varphi(\zeta,\varrho) = \psi_2(\varrho), \\ \varphi(\chi,0) = \psi_3(\chi), \end{cases} \tag{46}$$

where $\psi_1(\varrho)=0$, $\psi_2(\varrho)=\varrho^2\sin(1)$, and $\psi_3(\chi)=0$ are given from $\varphi(\chi,\varrho)=\varrho^3\sin(\chi)$. In problem 46, we compute the L_∞-norm of the absolute error for various values of the spectral parameters $\mathcal{M}$ and $\mathcal{N}$, with the results summarized in Table 1. This norm represents the maximum absolute error across the computational domain and provides a rigorous measure of the method's accuracy. Figure 1 presents the numerical solution $\hat{\varphi}(\chi,\varrho)$, visualized along both the ϱ-direction, and χ-directions. This figure highlights the behavior of the approximate solution across the domain and demonstrates its smoothness and consistency. Figure 2 displays the absolute error (AE) distribution for the case where $\mathcal{M}=\mathcal{N}=14$, illustrating the localized accuracy of the method. These error profiles confirm that the proposed RJSC technique maintains high accuracy throughout the domain, with only minor deviations near the boundaries. Furthermore, the convergence behavior of the method is depicted in Fig. 3, showing the decay of the error as the number of collocation points increases. The figure demonstrates the spectral convergence of the proposed scheme, where the error decreases exponentially with respect to the increase in $\mathcal{M}$ and $\mathcal{N}$.

Overall, the results indicate that the RJSC method delivers high-precision approximations even with a relatively small number of collocation points. This highlights its computational efficiency and suitability for solving distributed-order fractional convection-diffusion equations with excellent accuracy.

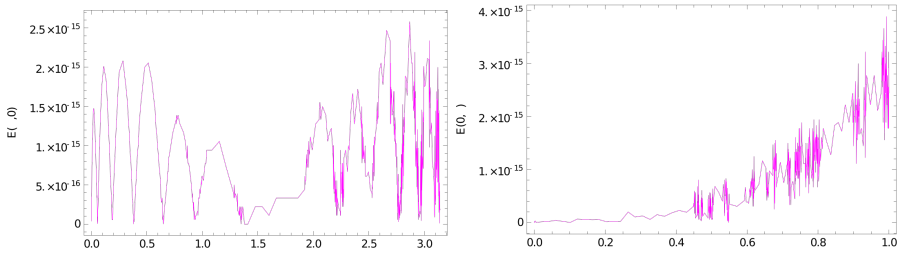

Fig. 1 – χ and ϱ-direction curve of the AEs problem 46 when $\mathcal{M} = \mathcal{N} = 14$ and $\epsilon = \frac{1}{2}$.

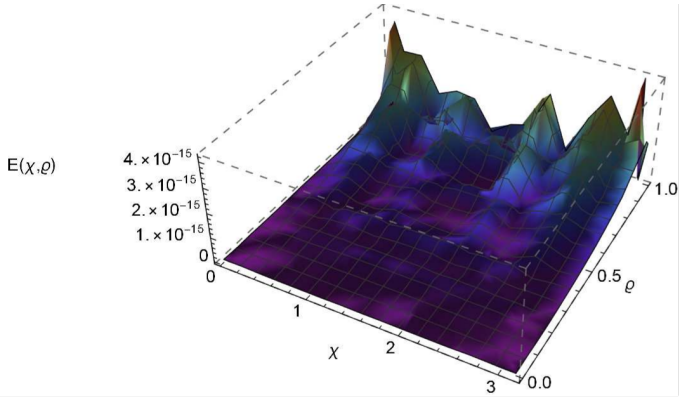

Fig. 2 – AEs for problem 46 for $\mathcal{M} = \mathcal{N} = 14$.

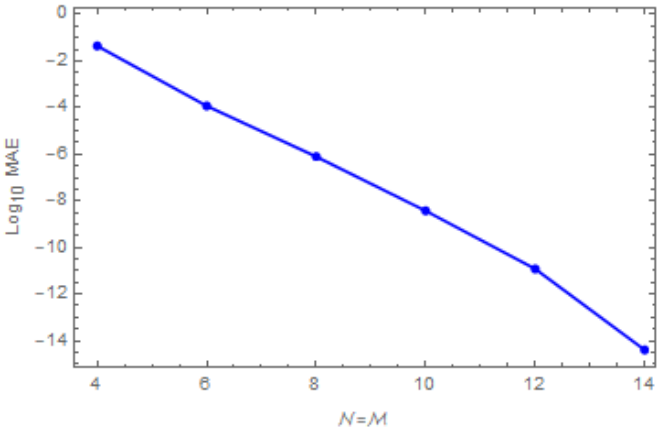

Fig. 3 – MAE convergence for problem 46 for difference of $\mathcal{M}, \mathcal{N}$.

5.2. TEST PROBLEM 2

We consider the non-linear DOFCDEs,

$$\begin{cases} \int_0^1 \aleph(\omega)\, {}^cD_{\varrho}^{\omega}\varphi(\chi,\varrho)\, d\omega - \frac{\partial^2\varphi(\chi,\varrho)}{\partial\chi^2} + \chi\frac{\partial\varphi(\chi,\varrho)}{\partial\chi} + \varphi(\chi,\varrho)^2 = \mathcal{F}(\chi,\varrho), \\ \varphi(0,\varrho) = \psi_1(\varrho), \\ \varphi(\zeta,\varrho) = \psi_2(\varrho), \\ \varphi(\chi,0) = \psi_3(\chi), \end{cases} \tag{47}$$

where $\psi_1(\varrho) = 0$, $\psi_2(\varrho) = 0$, and $\psi_3(\chi) = 0$ are given from $\varphi(\chi,\varrho) = \varrho^2(\chi^2 - \chi^3)$.

In problem 47, we evaluate the performance of the proposed RJSC method by computing the L_∞ -norm of the absolute error for different values of the spectral parameters. Specifically, for $\mathcal{M} = \mathcal{N} = 6$, the computed L_∞-error is 8.6518×10^{-12}, while for $\mathcal{M} = \mathcal{N} = 8$, the error is further reduced to 3.8832×10^{-14} . These results demonstrate the method's rapid convergence and high accuracy with relatively few collocation points.

Figures 4 and 5 illustrate the numerical solution $\hat{\varphi}(\chi,\varrho)$ of problem 47 along both the ϱ and χ-directions for $\mathcal{M} = \mathcal{N} = 6$ and $\mathcal{M} = \mathcal{N} = 8$, respectively. The plots confirm the stability and smoothness of the approximated solution as resolution increases.

Additionally, Fig. 6 presents the absolute error distribution for $\mathcal{M} = \mathcal{N} = 6$ and $\mathcal{M} = \mathcal{N} = 8$, providing a detailed view of the spatial accuracy of the method. The results confirm that the proposed RJSC approach achieves excellent precision even with a modest number of spectral collocation points, making it a highly efficient and accurate tool for solving distributed-order fractional convection-diffusion equations.

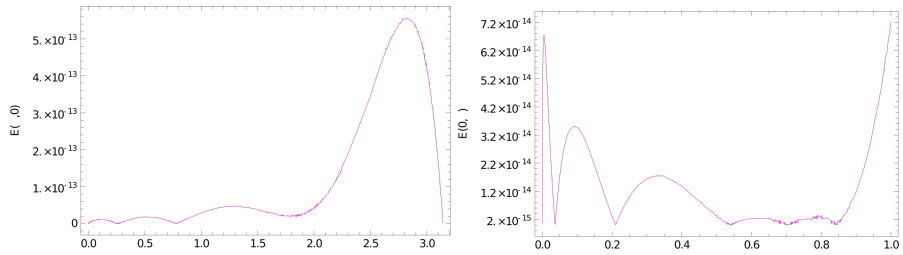

Fig. 4 – χ and ϱ-direction curve of the AEs problem 47 when $\mathcal{M} = \mathcal{N} = 6$.

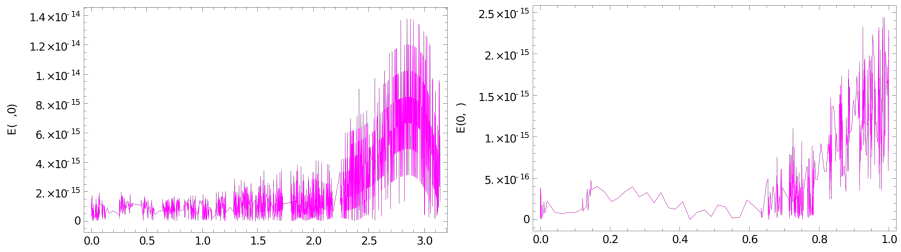

Fig. 5 – χ and ϱ-direction curve of the AEs problem 47 when $\mathcal{M} = \mathcal{N} = 8$.

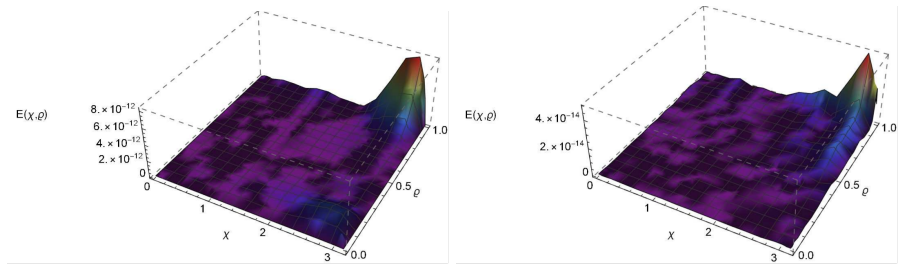

Fig. 6 – AEs for problem 47 for $\mathcal{M} = \mathcal{N} = 6$ and $\mathcal{M} = \mathcal{N} = 8$.

5.3. TEST PROBLEM 3

We consider the non-linear DOFCDEs,

$$\begin{cases} \int_0^1 \aleph(\omega)\, {}^cD_\varrho^\omega \varphi(\chi,\varrho)\, d\omega - \frac{\partial^2 \varphi(\chi,\varrho)}{\partial \chi^2} + x\frac{\partial \varphi(\chi,\varrho)}{\partial \chi} + \varphi(\chi,\varrho)^2 = \mathcal{F}(\chi,\varrho), \\ \varphi(0,\varrho) = \psi_1(\varrho), \\ \varphi(\zeta,\varrho) = \psi_2(\varrho), \\ \varphi(\chi,0) = \psi_3(\chi), \end{cases} \tag{48}$$

where $\psi_1(\varrho) = \varrho^2$, $\psi_2(\varrho) = \varrho^2 cos(1)$, and $\psi_3(\chi) = 0$ are given from $\varphi(\chi,\varrho) = \varrho^2 \cos(\chi)$.

In problem 48, the L_∞-norm of the absolute error is computed for various values of the spectral parameters $\mathcal{M}$ and $\mathcal{N}$, with the results presented in Table 2. These values demonstrate the high accuracy of the proposed RJSC method across different spectral resolutions. Figure 7 depicts the approximate solution $\hat{\varphi}(\chi,\varrho)$, of problem 48, visualized along both the ϱ, and χ–directions, highlighting the consistency and smoothness of the numerical approximation. The behavior of the solution is well captured by the RJSC method even at lower degrees of approximation. Figure 8 presents the absolute error (AE) distribution for the case $\mathcal{M} = \mathcal{N} = 14$, providing insight into the local accuracy of the solution throughout the domain. These error plots confirm the robustness and reliability of the proposed scheme. Furthermore, Fig. 9 illustrates

Table 2

The MAE for problem 48

$(\mathcal{M},\mathcal{N})$	MAE
$(2,2)$	3.87×10^{-1}
$(4,4)$	9.67×10^{-3}
$(6,6)$	1.31×10^{-4}
$(8,8)$	6.43×10^{-6}
$(10,10)$	5.76×10^{-9}
$(12,12)$	2.23×10^{-11}
$(14,14)$	6.43×10^{-14}

the convergence behavior of the method, showcasing the exponential decay of the error as the number of collocation points increases. These results clearly demonstrate that the RJSC method achieves high accuracy even with a relatively small number of collocation points, confirming its efficiency and suitability for solving complex distributed-order fractional convection-diffusion equations.

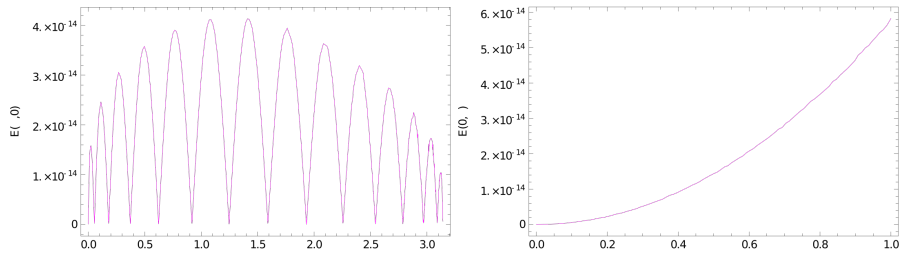

Fig. 7 – χ and ϱ-direction curve of the AEs problem 48 when $\mathcal{M}=\mathcal{N}=14$ and $\epsilon=\frac{1}{2}$.

5.4. TEST PROBLEM 4

We consider the 2D nonlinear DOFCDEs,

$$\int_0^1 \aleph(\omega)\,{}^cD_{\varrho}^{\omega}\varphi(\chi,\varrho,\xi)\,d\omega+\frac{\partial^2\varphi(\chi,\varrho,\xi)}{\partial\chi^2}+\frac{\partial^2\varphi(\chi,\varrho,\xi)}{\partial\varrho^2}+\frac{\partial\varphi(\chi,\varrho,\xi)}{\partial\chi}+\frac{\partial\varphi(\chi,\varrho,\xi)}{\partial\varrho}+\varphi(\chi,\varrho,\xi)^3=\mathcal{F}(\chi,\varrho). \tag{49}$$

The associated initial and boundary conditions (33) are extracted from the actual true solution $\varphi(\chi,\varrho,\xi)=\chi^2\xi^3(1-\chi)^2\varrho^2(1-\varrho)^2$.

Figure 10 presents the numerical solution $\hat{\varphi}(\chi,\varrho,\xi)$, visualized along both the ϱ-direction, and χ-directions. This figure highlights the behavior of the approximate

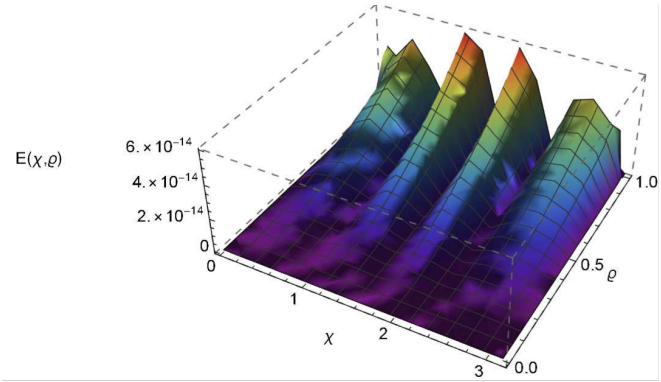

Fig. 8 – AEs for problem 48 for $\mathcal{M} = \mathcal{N} = 14$.

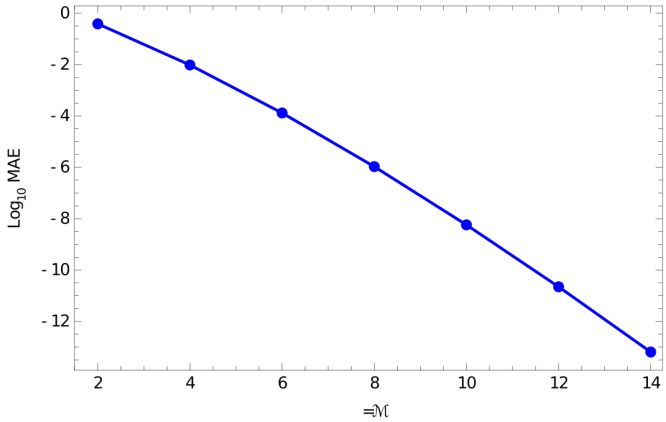

Fig. 9 – MAE convergence for problem 48 for difference of $\mathcal{M}, \mathcal{N}$.

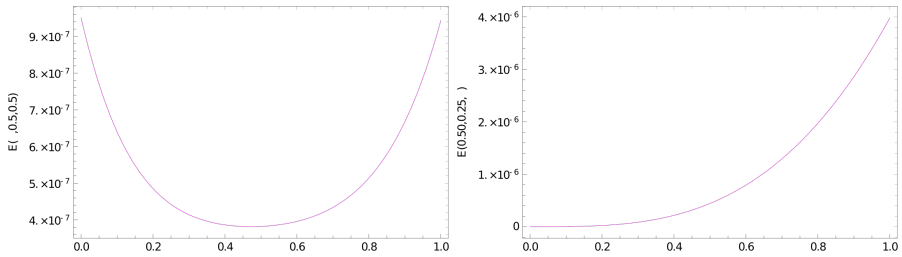

Fig. 10 – χ and ϱ-direction curve of the AEs problem 49 when $\mathcal{M} = \mathcal{N} = 12$ and $\epsilon = \frac{1}{2}$.

solution across the domain and demonstrates its smoothness and consistency. Figure 11 presents the absolute error (AE) distribution for the case $\mathcal{M} = \mathcal{N} = 12$, providing insight into the local accuracy of the solution throughout the domain. These error

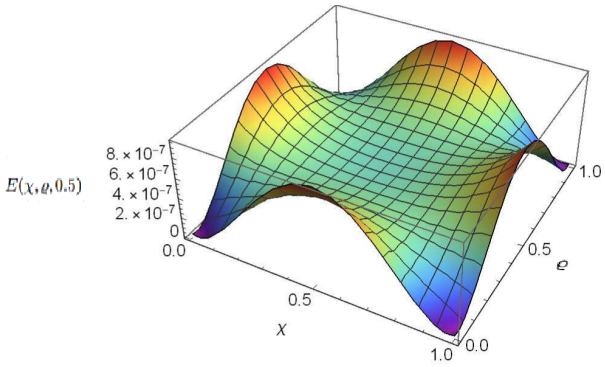

Fig. 11 – AEs for problem 49 for $\mathcal{M} = \mathcal{N} = 12$.

plots confirm the robustness and reliability of the proposed scheme.

6. CONCLUSION

This paper presents an accurate and efficient numerical technique for solving multi-dimensional non-linear distributed-order fractional convection-diffusion equations (DOFCDEs). The proposed method employs the Romanovski–Jacobi spectral collocation (RJSC) approach, which incorporates both initial and boundary conditions to construct high-fidelity spectral approximations. By evaluating the residuals at selected quadrature points and transforming the problem into a corresponding system of algebraic equations, the method achieves exceptional precision and computational efficiency. This advancement significantly enhances the numerical treatment of non-linear DOFCDEs, enabling the analysis of complex systems characterized by distributed-order dynamics across various scientific and engineering domains, including physics, biology, and engineering. The application of RJSC techniques marks a notable progression in the field of numerical analysis by offering a robust and flexible framework for addressing a wide class of fractional models. Moreover, the rigorous computation of residuals at collocation nodes ensures that the approximate solution closely captures the intrinsic behavior of the underlying physical system. This level of accuracy is essential in contexts such as technical design, scientific modeling, and risk assessment, where reliable and precise solutions are critical.

Acknowledgements. This work was supported and funded by the Deanship of Scientific Research at Imam Mohammad Ibn Saud Islamic University (IMSIU) (grant number IMSIU-DDRSP2502).

REFERENCES

1. B. I. Henry, T. A. M. Langlands, P. Straka, Phys. Rev. Lett. **105**, 170602 (2010).

2. A. W. Leung, *Systems of Nonlinear Partial Differential Equations: Applications to Biology and Engineering*, **49**, Springer Science and Business Media, 2013.
3. D. S. Jones, M. Plank, B. D. Sleeman, *Differential Equations and Mathematical Biology*, 2nd edn., Chapman and Hall/CRC, New York, 2009.
4. J. Cruz, M. Grossinho, D. Sevcovic, C. I. Udeani, arXiv:2207.11568 (2022).
5. T. Eftekhari, J. Rashidinia, K. Maleknejad, Adv. Differ. Equations **2021**, 461 (2021).
6. A. Z. Amin, M. A. Abdelkawy, E. Solouma, I. Al-Dayel, Fractal and Fract. **7**(11), 780 (2023).
7. B. A. Malomed, Chaos **34**, 022102 (2024).
8. Guo-Qing Liu, Guo-Cheng Wu, Rom. J. Phys. **69**, 107 (2024).
9. H. O. Sidi, M. Babatin, M. Alosaimi, A. S. Hendy, M. A. Zaky, Rom. Rep. Phys. **76**, 104 (2024).
10. A. W. Alrowaily, R. Shah, A. H. Salas, W. Alhejaili, C. G. L. Tiofack, S. M. E. Ismaeel, S. A. El-Tantawy, Rom. Rep. Phys. **76**, 112 (2024).
11. D. Mihalache, Rom. Rep. Phys. **76**, 402 (2024).
12. X. Li, H. Rui, Appl. Numer. Math. **131**, 123-139 (2018).
13. W. Bu, A. Xiao, W. Zeng, J. Sci. Comput. **72**, 422-441 (2017).
14. W. Bu, L. Ji, Y. Tang, J. Zhou, Appl. Numer. Math. **152**, 446-465 (2020).
15. X. Gao, F. Liu, H. Li, Y. Liu, I. Turner, B. Yin, Comput. Math. Appl. **80**(5), 923-939 (2020).
16. W. Qiu, D. Xu, H. Chen, J. Guo, Comput. Math. Appl. **80**(12), 3156-3172 (2020).
17. A. Nouy, Arch. Comput. Methods Eng. **16**(3), 251-285 (2009).
18. M. A. Abdelkawy, M. J. Begum, A. S. Alnahdi, T. M. Taha, E. M. Soluma, Boundary Value Probl. **2022**, 1-15 (2022).
19. M. Abbaszadeh, M. Dehghan, Numer. Algorithms **75**, 173-211 (2017).
20. Q. Liu, S. Mu, Q. Liu, B. Liu, X. Bi, P. Zhuang, B. Li, J. Gao, Eng. Anal. Bound. Elem. **96**, 55-63 (2018).
21. G.-h. Gao, Z.-z. Sun, Numer. Algorithms **74**, 675-697 (2017).
22. G.-h. Gao, H.-w. Sun, Z.-z. Sun, J. Comput. Phys. **298**, 337-359 (2015).
23. H. Chen, S. Lü, W. Chen, J. Comput. Phys. **315**, 84-97 (2016).
24. M. H. Heydari, Results Phys. **51**, 106750 (2023).
25. P. Rahimkhani, Y. Ordokhani, P. M. Lima, Appl. Numer. Math. **145**, 1-27 (2019).
26. S. Saifullah, A. Ali, Z. A. Khan, AIMS Math. **7**(4), 5275-5290 (2022).
27. M. A. Abdelkawy, A. Z. M. Amin, A. M. Lopes, Comput. Appl. Math. **41**(1), 2 (2022).
28. A. Z. Amin, A. M. Lopes, I. Hashim, Int. J. Nonlinear Sci. Numer. Simul. **2022**(5), 1613-1630 (2022).
29. A. Amin, M. Abdelkawy, A. Amin, A. M. Lopes, A. Alluhaybi, I. Hashim, AIMS Math. **8**, 20871-20891 (2023).
30. E. H. Doha, M. A. Abdelkawy, A. Z. M. Amin, D. Baleanu, Nonlinear Anal. Model. Control **24**(3), 332-352 (2019).
31. E. Kharazmi, M. Zayernouri, G. E. Karniadakis, SIAM J. Sci. Comput. **39**(3), A1003-A1037 (2017).
32. F. Fakhar-Izadi, M. Dehghan, Math. Methods Appl. Sci. **36**(12), 1485-1511 (2013).
33. E. H. Doha, M. A. Abdelkawy, A.Z.M. Amin, A.M. Lopes, Commun. Nonlinear Sci. Numer. Simul. **72**, 342-359 (2019).
34. M. Izadi, P. Veeresha, W. Adel, Eur. Phys. J. Plus **139**(3), 205 (2024).
35. J. Nazari, M. H. Heydari, M. Hosseininia, Results Phys. **53**, 106937 (2023).